The Characteristics of Curved Wall Power Fluidics

The Characteristics of Curved Wall Power Fluidics

Osamu KINOSHITA* and Masao MURAKAMI**

(Received June 15, 1979)

This experimental investigation was conducted to obtain the effects of the curved side walls necessary for development of the more efficient power fluidic device. Three types of side wall used were (1) the straight wall (SW), (2) the curved wall which was based on the attachment stream line (AW) and (3) the circular arc wall whose radius was smaller by the half nozzle width than the radius of center stream line (CW). Using water of about 20°C as the operating fluid, the experimental studies were performed under the various conditions. The important results obtained were concerned with the output or the input characteristics, the output or input switching characteristics, output noise, the flow recovery, the power recovery and so on. AW element was more improved on various characteristics than SW element. CW element was almost the same with AW element.

1. Introduction

Power fluidics has promising areas of application such as diverting valves and thrusters. Straight wall devices generally used are attended with the vortex in the attached side. Though the vortex stabilizes the attachment jet from various disturbances, it causes vortex loss whose defect cannot be afforded to overlook. In order to make the affection of vortex to performance characteristics clear and also to develop the more efficient liquid power fluidics, the basic experimental investigation of water jet has been reported[1]. In this investigation the authors use curved wall devices as the experimental model for the purpose of making vortex loss slight.

The effects of the curved wall devices have been investigated by T. Sarpkaya[2]. The curved wall used in his research consists of an adequate circular arc based on the attachment stream line. K. Tsuchiya et al[3] have studied and discussed on the characteristics of their waved side wall devices. These investigations are unique and good examples of curved wall fluidics, however, they seem to leave many problems to be solved. Referring to their leading works, the authors study the static characteristics of the curved wall devices. Three kinds of side wall used are (1) the straight wall (SW), (2) the curved wall which is based on the attachment stream line (AW) and (3) the circular arc wall whose radius is smaller by the half nozzle width than the radius of the center stream line (CW).

The objects of this investigation are:

1. The static effects of the curved wall on performance characteristics such as the output or input characteristics, the output or input switching characteristics, output noise, the flow recovery and the power recovery and so on.

* Course of Mathematics and Related Fields, College of Integrated General Arts and Sciences.
** Institute of Industrial Sciences, University of Tokyo.

2. The development or the suggestion of the more efficient liquid fluidic devices.

2. Experimental Equipment and Procedure

Fig. 1 shows a schematic diagram of the experimental apparatus. The experimental model was set horizontally at a depth of 15 cm in the water pool and was driven by water of about 20°C supplied from the head thank of 2.5 m height. The static pressures at various measuring points were measured by water or mercury manomenters. The main jet and control flow were regulated by valves and the main jet velocity at the nozzle exit v_s as well as the dimensionless control flow Q_c/Q_s (Q_s: main jet supply flow) were varied as follows: v_s = 2.0 – 3.0 m/s [Reynolds number Re = (4.0 – 6.0) x 10^4] and Q_c/Q_s = 0 – 0.5. These average flow rates were measured by means of orifices and mercury manometers.

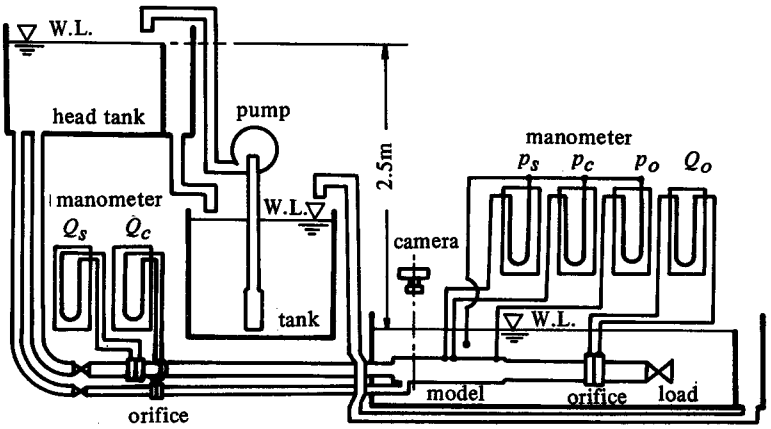

Fig. 1. Schematic diagram of experimental set up.

2.1 Experimental model

The experimental model used for investigation of the effects of the curved wall is as shown in Fig. 2. The figure shows the straight wall model which is the basis of the curved wall element. The attachment stream line and the center stream line were measured by flow visualization which was done utilizing the air bubble tracer. The air bubbles were generated by blowing vinyl tubes connected to injection syringes (outer diameter: 0.2 mmϕ) which were set near the main nozzle exit. The air bubbles mixed in the stream were illuminated by parallel ray of about 0.5 mm thickness which was projected through the side wall of the model from a narrow slit placed in a slide projector. The trajectories of sparkling bubbles were photographed. This visualization method is very simple even though care must be taken not so as to affect the liquid specific gravity as well as the pressure distribution in the model.

The shape and position of the splitter are based on the suggestion by M. Ohta et al[4].

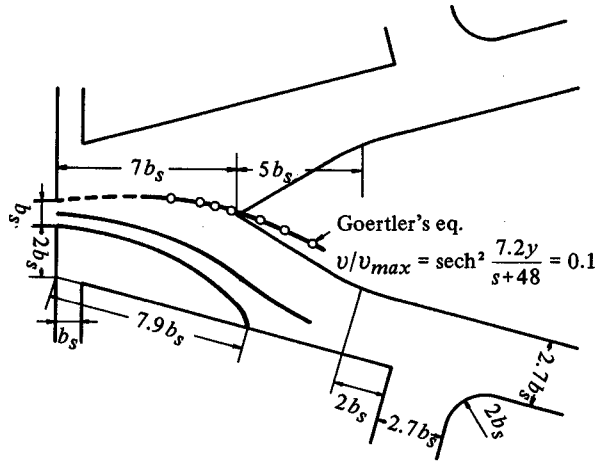

Fig. 2. Experimental model.

The spread parameter on the unattached side σ and the distance from the nozzle exit to the hypothetical point source of the jet s_o were obtained in the case without the splitter as $\sigma = 7.2$ and $s_o = 48$ mm[1]. Therefore the Goertler's distribution is expressed as

$$v/v_{max} = \text{sech}^2 [7.2y/(s+48)] \tag{1}$$

where v: flow velocity in s direction, v_{max}: maximum velocity, y: perpendicular distance from jet maximum velocity line, s: distance from nozzle exit measured along jet center line. The velocities calculated from this equation are slightly larger than the experimental data at the tail end. Then the outer boundary stream line on the unattached side is assumed to be

$$v/v_{max} = \text{sech}^2 [7.2y/(s+48)] = 0.1 \tag{2}$$

This is plotted in Fig. 2. This curve passes near by the tip of the splitter which is located with the splitter distance of $7b_s$.

This principal dimensions are:
main nozzle width b_s (= control nozzle width b_c): 20 mm, offset D: $2b_s$, side wall angle: 15°, aspect ratio: 6.2 and output port width (= vent width): $2.7b_s$.

2.2 Curved walls

Fig. 3 shows three kinds of wall configurations used for the experiments. These are:

1. Straight wall (SW).
2. Attachment stream line wall (AW).
   This type of wall configuration is based on the attachment stream line. The real curve is offset by $0.1b_s$ considering the spread of the jet at the control port edges and has modification of the attachment stream line by the adequate smooth stream line near the attachment point in order to avoid the loss of impingement.

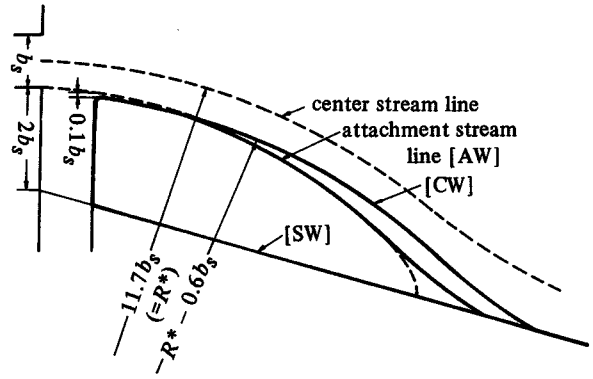

Fig. 3 Three types of side wall.

3. Center stream line wall (CW).

This type of wall configuration is based on the center stream line obtained by flow visualization in case of the straight wall model with the splitter set at the predetermined position. The configuration of the center stream line is almost regarded as circular arc. The radius of curvature of the center stream line R^* is measured as $11.7b_s$. Considering the spread of the jet $0.1b_s$ alike the case of AW and a half of the main nozzle width $0.5b_s$, the radius of curvature $(R^* - 0.6b_s)$ is adopted. Near the attachment point the modified curve in the case AW is also adopted.

The experiments were done using three kinds of wall configurations, namely, SW, AW and CW. During the experiments the control nozzle on the unattached side was always closed.

3. Experimental Results

3.1 Output characteristics

Figs. 4(a) and (b) show the experimental results with respect to the output characteristics in the cases with and without the vent respectively. The output flow Q_o and the output static pressure p_o are normalized by the supply flow Q_s and the supply total pressure P_s respectively. The data were obtained in three cases where the main nozzle exit velocity v_s was equal to 2.0, 2.5 and 3.0 m/s. Fig. 4(a) indicates that the maximum pressure recovery in case of SW is 0.31 and those in cases of AW and CW are 0.41 and 0.49 respectively. Therefore it can be said that the curved walls improve the maximum pressure recovery.

In the cases without the vent shown in Fig. 4(b) switching occurs in every wall configuration when the load is increased, but the insensitiveness to the load pressure varies according to the wall configuration. As observed from the figure, AW gives the best insensitiveness that is maximum pressure ratio = 0.4 and minimum flow rate = 0.4. It should be noted that the flow separation is hard to occur even under the severe condition

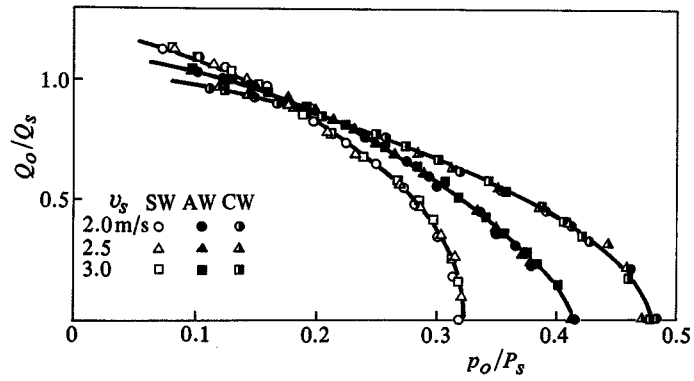

(a) Vented

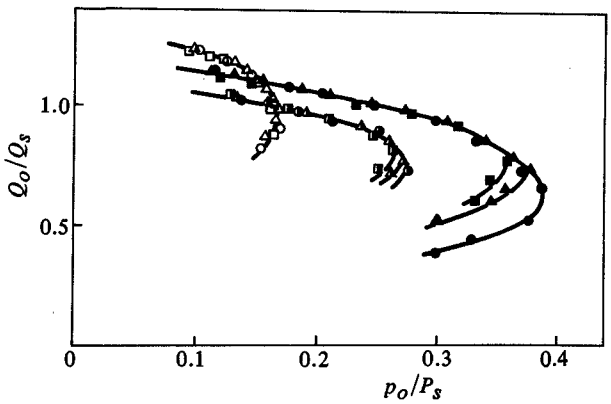

(b) Unvented

Fig. 4. Output characteristics.

when the shape of the side wall fit properly the attachment stream line such as AW element. In every case switching does not occur at the maximum of p_o/P_s but occurs when p_o/P_s becomes smaller.

3.2 Input characteristics

Input characteristics is defined as the relationship between the control flow Q_c and the control static pressure p_c. Q_c and p_c are normalized by Q_s and p_s respectively. Fig. 5 shows the input characteristics. In order to be available to consider the fanout, the control static pressure p_c was measured at the position upstream of the control nozzle where the control port width becomes the same with the output port width (= $2.7b_s$). When the control pressure and flow are increased, the switching occurs. As observed from the figure, the switching point in the case of SW is $p_c/P_s = -0.12$ and $Q_c/Q_s = 0.24$; that in the case of AW is $p_c/P_s = -0.75$ and $Q_c/Q_s = 0.01$; and that in the case of CW is $p_c/P_s = -1.20$ and $Q_c/Q_s = 0.01$. The difference in the input cha-

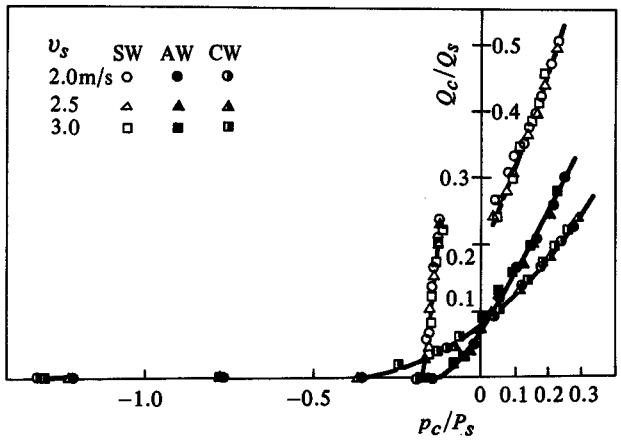

Fig. 5. Input characteristics.

racteristics of the three elements seems to be caused by the difference in bias pressures of the unattached control ports and the difference in the input resistances. The slope of the curves after switching in the cases of the curves walls are more gentle than that in the case of the straight wall. Since switching occurs at quite small control flow ratio such as 0.01 in the cases of the curved wall, it can be said that the curved walls improve the sensitivity to the input.

3.3 Output switching characteristics

Fig. 6 shows the experimental results of the output switching characteristics. These

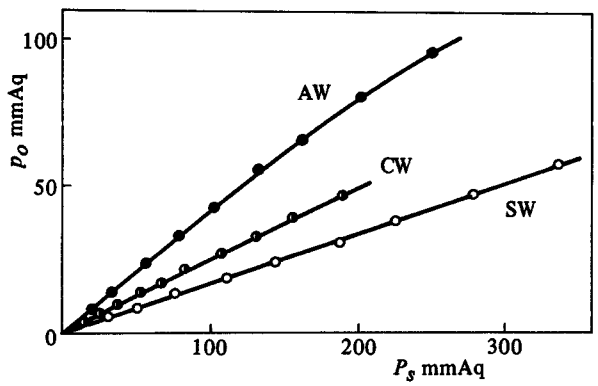

Fig. 6. Output switching characteristics.

characteristics are concerned with the unvented cases. The maximum output pressures at which switching does not occur are obtained for various supply pressures in the cases of three wall configurations. As described in connection with Fig. 4(b), switching occurs when the output pressure begins to decrease after it reaches the maximum point. There-

fore the maximum output pressure can be taken as the measure of insensitiveness to the load. The curved walls are superior to the straight wall in this connection. Comparing two curved walls AW is better than CW. This may be because the separation bubble is apt to occur in the downstream region of the convex in case of CW.

In order to know the switching mode by output load, internal flow was observed by means of the tracer method [Figs. 7(a) and (b)]. In the case of SW element, when the

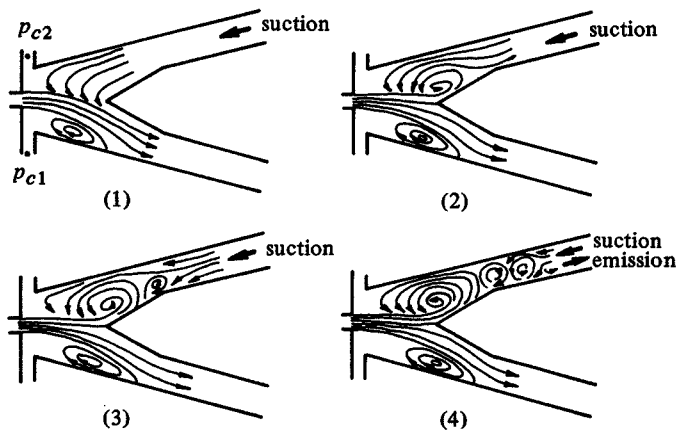

(a) Straight wall model.

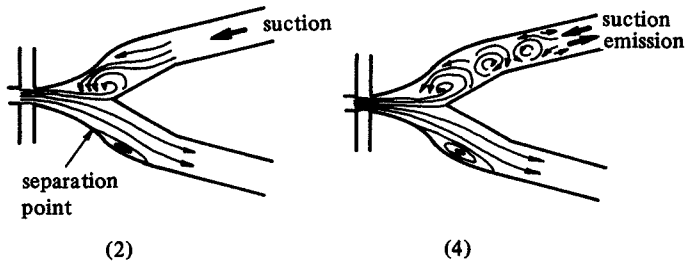

(b) Curved wall model.

Fig. 7. Flow patterns.

output load increases the attachment vortex becomes larger and the center of the vortex together with the attachment point moves downstream, that is, the separation of the jet grows toward downstream region. Therefore the curved jet becomes to be straightened and then to be switched. In the case of the curved wall element such as AW or CW, when the load increases the separation vortex occurs in the downstream region of the convex wall, and then the vortex becomes larger and grows toward downstream region.

3.4 Input switching characteristics

Fig. 8 shows the experimental results of the input switching characteristics. In this figure the data expressed by small circles are the static pressure of the control port at

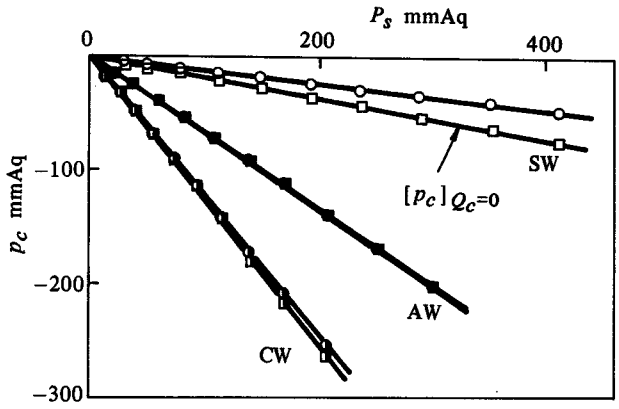

Fig. 8. Input switching characteristics.

switching and the data expressed by small squares are those when the control flow is zero. When the control flow Q_c is increased, the static pressure of the control port p_c rises and approaches the curves connecting the data expressed by small circles and then switching occurs when these curves are reached. As mentioned previously and observed from the figure, the curved walls are superior to the straight wall in this connection. Comparing two curved walls, the switching occurs when both control flows are almost same (Q_c/Q_s = 0.01), but when concerning the control static pressure CW is lower than AW.

3.5 Output noise

In connection with the output noise, the velocity fluctuation v' in the direction of average flow was measured on the middle region between the upper and lower walls at the output port exit. Measurements were done using a constant temperature hot film anemometer which calibrated enough in regard to water temperature and velocity. In Fig. 9 the experimental results of the average velocity distributions v_{out} (the three lines in the right hand side) and the output noise concerned with the velocity fluctuation (the three kinds of data in the left hand side) are shown. As observed from three lines in the right hand side of the figure, three average velocity distributions are not flat such that all of them are larger in the attached side, while the average velocity of vertical distributions between the upper and the lower wall are almost flat. In spite of the same nozzle velocity (v_s = 3.0m/s), three distributions become wholly smaller in order of SW, AW and CW, because the volumes of entrainment flow become smaller in the same order.

The fluctuation intensities in the output flow of the curved wall elements such as AW and CW are almost same ($\sqrt{\overline{v'^2}}/v_{out} = 0.1$). Generally speaking, fluctuation intensity of jet ejected in still water is about 0.3 – 0.4. As observed from the figure the turbulence

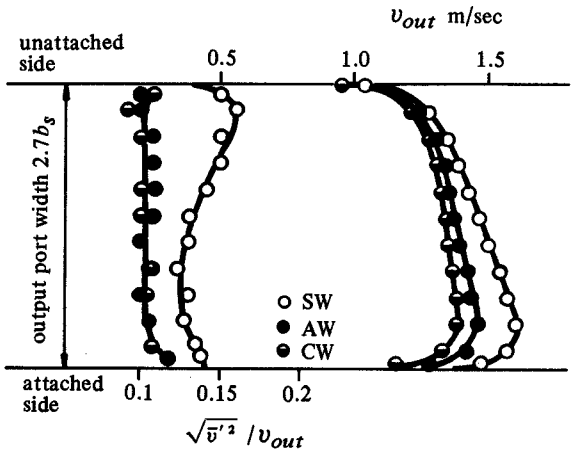

Fig. 9. Velocity and fluctuation profiles in the output port.

attenuates in the output port as the flow goes downstream. The difference of the fluctuation in AW or CW element from that in SW element is based on the difference of occurrence, for the attenuations of AW or CW and SW seem to be equal in the same output port.

3.6 Flow recovery

The flow recovery is defined as the ratio of the output port flow volume Q_o and the main nozzle flow volume Q_s when the output port valve is fully open. The relation of the flow recovery Q_o/Q_s and Reynolds number Re are shown in Fig. 10 with or without vent. All flow recoverys under various conditions are unchanged concerned with

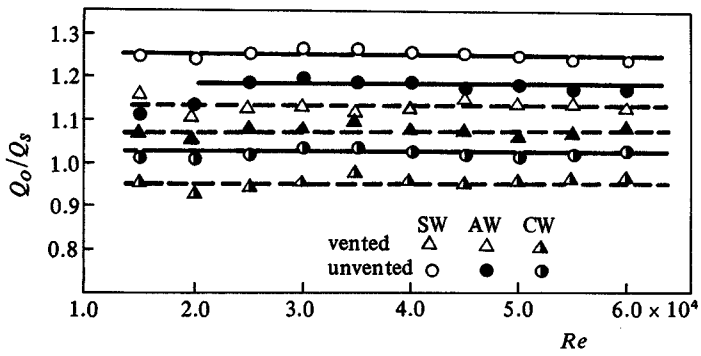

Fig. 10. Flow rate recovery versus Re-number.

Reynolds number. The flow recoveries are smaller in order of SW, AW and CW, while this order is opposite to that of maximum output pressures in Fig. 4(a). Therefore an element of higher pressure recovery tends to be a lower flow recovery element.

3.7 Power recovery

Fig. 11 shows the experimental results of the power recovery. Let P_o be the total pressure of output port when the output port valve is fully open and Q_o be the output flow at that time; then the power recovery is defined as the ratio of P_oQ_o to the supply

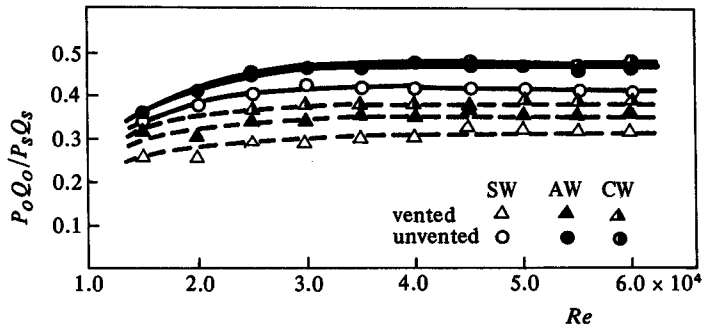

Fig. 11. Power recovery versus Re-number.

power P_sQ_s. The figure shows how the power recovery varies in accordance with the Reynolds number Re in cases of three wall configurations and in cases with and without the vent. The power recoveries in the unvented case of AW and CW are almost equal and around 0.48. This is higher by 0.07 than the case of the straight wall element. The advantage of the curved walls is that the vortex loss is very small. However the entrainment in the cases of the curved walls is smaller than that in the case of the straight wall. This will be the reason why the power recoveries in the cases of the curved walls are not so improved compared with the straight wall. A significant difference can not be observed between AW and CW. The fact that the power recoveries in the vented cases are smaller than those in the unvented cases is due to the outflow through the vent.

Consider the power recovery depends on any factors. Let p_s (=total pressure P_s) be the supply static pressure where the velocity can be neglected at the upstream region of the main nozzle, Q_s be the supply flow, Q_o be the output flow and p_e be the average static pressure at the main nozzle exit. Observing the pressure distributions near the main nozzle exit[1] and the flow recovery of Fig. 10, two equations are found to be as follows.

$$p_e = -K_p \cdot p_s \tag{3}$$

$$Q_o = K_q \cdot Q_s \tag{4}$$

where K_p and K_q are the pressure coefficient and flow coefficient respectively.

The supply flow Q_s can be determined by Bernoulli's law with the nozzle discharge

coefficient α and the sectional area of nozzle exit f_n, so that

$$Q_s = \alpha f_n [2g(p_s - p_e)]^{1/2} = \alpha f_n [2g(1 + K_p)p_s]^{1/2} \tag{5}$$

Since the velocity can be neglected at p_s measuring point, $p_s = P_s$; then the supply power $P_s Q_s$ is

$$P_s Q_s = Q_s^3 / [\alpha^2 f_n^2 2g(1 + K_p)] \tag{6}$$

When the static pressure at the output port exit is regarded as atmospheric pressure and the sectional area of the output port is f_o, the total output pressure P_o is given from Eq. 4, therefore

$$P_o = (K_q \cdot Q_s)^2 / 2g f_o^2 \tag{7}$$

Then the output power $P_o Q_o$ is

$$P_o Q_o = (K_q^2 Q_s^2 \cdot K_q Q_s)/2g f_o^2 = (K_q^3 \cdot Q_s^3)/2g f_o^2 \tag{8}$$

From Eqs. 6 and 8, the power recovery is induced as follows:

$$P_o Q_o / P_s Q_s = \alpha^2 (f_n / f_o)^2 K_q^3 (1 + K_p) \tag{9}$$

In Eq. 9 the factors α, (f_n/f_o), K_q and K_p vary in connection with each other. In the study (f_n/f_o) as well as α are constant. K_q and K_p can be varied. When the offset or the side wall angle decreases the attachment vortex moves upstream and vortex pressure falls; then K_p increases. However, K_q becomes smaller, since the entrainment flow decreases. K_p and K_q changes in the opposite way.

Substituting these data for Eq. 9 the power recoverys are calculated as 0.42 (SW), 0.51 (AW) and 0.47 (CW). These values almost agree with the experimental data of Fig. 11.

4. Conclusions

This paper presents the characteristics of curved wall elements. Three types of side wall used are (1) straight wall (SW), (2) the curved wall which is based on the attachment stream line (AW) and (3) the circular arc wall whose radius is smaller by the half nozzle width that the radius of center stream line (CW).

Using water of about 20°C as the operating fluid, the experimental studies were performed under the conditions of main jet velocity $v_s = 2.0 - 3.0$ m/s and dimensionless control flow rate $Q_c/Q_s = 0 - 0.5$ (Q_s : supply flow rate). The following experimental results are obtained:

(1) SW elements has the only merit that the flow recovery is better than the others. The primary weak point of this type is troubles due to the vortex. The vortex loss causes decrease of pressure recovery and power recovery. The vortex oscilla-

tion results in instability for load and noisy output flow. Input sensitivity is also low.

(2) AW element is more improved on various characteristics except flow recovery than SW element. The vortex is replaced with side wall, so that pressure recovery, power recovery, stability and output flow condition are better. Input sensitivity is very high.

(3) CW element is almost the same with AW element with regards to power recovery and input sensitivity. But approximation of attachment stream line to circular arc affects the other characteristics slightly.

References

1) Y. Oshima and O. Kinoshita, Proc. of the IFAC 6th World Congress, Boston, Part 4 (1975).
2) T. Sarpkaya, Jou. of Basic Engineering, 91, 2, (1969).
3) K. Tsuchiya, H. Oda, T. Ishihara and H. Kondo, Proc. of 8th National Fluidics Symposium, Okayama, (1973).
4) M. Ohta, H. Matsuo and M. Kiuchi, Proc. of 3rd National Fluidics Symposium, Kyoto, (1968).